We are IntechOpen, the world's leading publisher of Open Access books Built by scientists, for scientists

4,800
Open access books available

122,000
International authors and editors

135M
Downloads

Our authors are among the

154
Countries delivered to

TOP 1%
most cited scientists

12.2%
Contributors from top 500 universities

CLARIVATE ANALYTICS BOOK CITATION INDEX INDEXED

WEB OF SCIENCE™

Selection of our books indexed in the Book Citation Index in Web of Science™ Core Collection (BKCI)

Interested in publishing with us?
Contact book.department@intechopen.com

Numbers displayed above are based on latest data collected.
For more information visit www.intechopen.com

13

The Thermodynamics of Defect Formation in Self-Assembled Systems

Colm T. O'Mahony, Richard A. Farrell, Tandra Goshal, Justin D. Holmes and Michael A. Morris
The Tyndall National Institute and University College Cork and CRANN, Trinity College Dublin Ireland

1. Introduction

The self-assembly of matter into highly ordered structures at the nanometer scale or beyond, is a topic that has attracted significant research over the past two decades. The term self-assembly is used to describe spontaneous processes where nanoscale entities pack into regular arrangements in order to attain a minimum free energy through minimisation of repulsive and maximisation of attractive molecular interactions (Whitesides & Grzybowski, 2002). Note that in most self-assembly processes, the formation of regular arrangements are enthalpy driven but in certain circumstances, entropy driven processes can produce ordered arrangements as discussed briefly below. These pattern formed in a self-assembly process have potential importance, as they may provide techniques to generate nanostructured surfaces by a simple, cost-effective method as opposed to current, expensive lithographical processes. The formation of these 'self-assembled' structures is thermodynamically driven and derived from the lower free energy of the structured, assembled system compared to that of the random structure. The lower free energy is usually a result of weaker intermolecular forces between, assembling or organising, moieties and is essentially enthalpic in nature. Pattern formation is a thermodynamic comprise between pattern generation, rate of pattern formation and the degree of disorder (Whitesides & Mathis, 1991).

Disorder can arise in self assembled systems in two ways; intrinsic and extrinsic sources. Thermodynamically intrinsic defect formation is defined by the entropy of a system and the free energy of defect formation. Disorder can also occur from kinetically derived extrinsic defects arising from mass-transport imitations in pattern formation. Extrinsic defects can also arise from contamination, moiety size irregularities, substrate effects, mechanical damage, etc. Understanding defect formation, the resultant density and control of defect concentrations is of critical importance is the possible application of these materials. The term self-assembly has also been applied to processes not involving individual entities but also has been used to describe processes such as phase separation within a single component (as in the example described here, block copolymer (BCP) microphase separation, and this is discussed in depth below). Phase separation can probably be more correctly described by the related term self-organisation. The difference between self-

assembly and self-organisation can be difficult to differentiate (Misteli, 2001) and this is given consideration below. Very often in chemistry self-assembly and self-organisation are used interchangeably and we will continue this practice in this article. As more explicitly stated below, self-assembly is generally reserved for systems that are driven to equilibrium via physical interactions between entities (a free energy minimum). Self-organisation refers to a dynamic process where the assembled or organised structure is in a steady state. In block copolymer self-assembly, the interactions between different blocks results in a free energy minimum for specific ordered arrangements of the chains. These structures have a nano-dimension (i.e. the same scale as the polymer blocks) because complete phase separation cannot occur because of the bonds between blocks. For BCP systems, a well-defined order-disorder transition is present defined by a temperature where the chains are too mobile to form discrete ordered arrangements. As described below, these systems reach a true equilibrium and the term self-assembly can be properly used as outlined further below.

1.1 Self-assembly

Self-assembly is an equilibrium process that represents a balance between repulsive and attractive forces between entities. These forces are manifest as a minimum in potential energy with distance apart and are discussed further below. This provides a useful framework for understanding and modelling the microphase separation of BCPs. The thermodynamics of the self-assembly process can be represented by a simple Gibbs Free Energy equation:

$$\Delta G_{SA} = \Delta H_{SA} - T\Delta S_{SA} \quad (1)$$

where self-assembly is a spontaneous process if ΔG_{SA} is negative. ΔH_{SA} is the enthalpy change of the process and is largely determined by the potential energy/intermolecular forces between the assembling entities. ΔS_{SA} is the change in entropy associated with the formation of the ordered or hierarchical arrangement. Since the organisation is generally (but not always) accompanied by an entropy decrease, for self-assembly to be spontaneous the enthalpy term must be negative and in excess of the entropy term. The equation shows that the self-assembly process will become progressively less likely as the magnitude of $T\Delta S_{SA}$ approaches the magnitude of ΔH_{SA} and above a critical temperature, spontaneous self-assembly will not occur. Note, that in many examples of self-assembly it may be more useful to think about self-assembly bringing about a reduction of the Helmoltz free energy since reactions are carried out in closed reaction cells.

Self-assembly is a classic example of thermodynamics. In thermodynamic terms, self-assembly is due to the minimization of free energy in a closed system and the result is an equilibrium state (Jones, 2004). In systems which are enthalpy driven and entropy appears to decrease, there is no contravention of the Second Law of Thermodynamics when the whole of the system rather than the aggregation moieties is considered. In a self-assembly process, individual lower thermodynamically stable species are used to generate more thermodynamically stable aggregates at a higher hierarchical level. The reaction proceeds via temporal changes within the system such as diffusion and other forms of mass transport which allow the aggregated self-assembled structure or a precursor there of to be 'sampled'. The lifetime (τ) of the aggregated structure is given by and equation of the form such as:

$$\tau = \tau_o \, (\exp \, (\Delta G_{SA}/RT)) \quad (2)$$

where τ_o represents the average time between collisions or vibrations or similar events that may lead to dissociation of the aggregate. This is an important equation because it suggests that although these self-assembled arrangements may be experimentally observed microscopically, spectroscopically and structurally, they may be in constant flux and changing during the observation. It is, of course, an absolute pre-requisite that the system is in some sort of flux because of the nature of the equilibrium process. The individual components (molecules, particles, polymer chains etc.) must 'sample' the organised structure for the self-assembly process to occur. Kinetic energy is thus an important parameter in a self-assembling system. If it is too low, the rate of formation of the organised structure will be to low to be practical. If it is too high, the organised structure will not form. Understanding the self-assembly is a fundamental challenge in modern science. It is at the very heart of nature and is responsible for all life and the thermodynamics of this process have been considered in depth not only scientifically but form a more philosophical view (Bensaude-Vincent, 2009).

It should also be noted that not all self-assembly processes are examples of simple thermodynamics. Self-assembly can result in metastable states whose form is dependent on an external source of energy. This is often described as dynamic self-assembly. Temperature, magnetic fields, chemical reactions, light etc. can be used to select or modify the metastable states that are formed (Grzybowski et al., 2009). The term dynamic self-assembly was coined by Whitesides and Grzybowski (Whitesides and Grzybowski, 2002). However, the definition they used is more applicable to the use of the term self-organisation. Self-assembly, certainly in the field of nanotechnology, has been used interchangeably with self-organisation but it is becoming clear that an exact differentiation between these is necessary at least in the biological field Halley and Winkler, 2008). Halley and Winkler outline the main distinctions between these two processes that can result in the formation of well-organised patterns from smaller entities. Firstly, whilst self-assembly is a true equilibrium process, self-organisation is not and requires an external (to the system) energy source. It is this definition that defines the term dynamic self-assembly as a true self-organisation phenomenon. It should be noted that practically the two processes can be separated experimentally because the organisation decays one the energy source is terminated. Secondly, self-assembly produces a well-defined, stable structure determined by the components of the system and the interactions between them whilst self-organisation is more variable with the structures being less stable and prone to change (Gerhart and Kirschner, 1997). Finally, self-assembly can be associated with a very limited number of components but in self-organisation there is a much higher number of components below which the organisation cannot occur (Nicholas and Prigogine, 1995). Whilst, the definition described here seems clear cut, this remains an area of considerable debate and arguments for the foreseeable future will continue.

It was suggested that above that generally, self-assembly is an enthalpy driven process. This is certainly true for work described in the area of nanotechnology on which this article focuses. However, in biology as well as a few examples in materials science, self-assembly is entropy not enthalpy driven. This may seem counter-intuitive but is well known and documented for systems such as micelles (Capone et al., 2009), some liquid-crystal molecules and colloidal particles (Adams et al., 1998) as well as various biological systems such as viruses (Frared et al., 1989). The reason the entropy increase favours more organised structures is because these structures allow more degrees of freedom within the system. E.g. increased rotation when rod-like structures are arranged parallel to one another rather than in an entanglement or increased degrees of freedom or water molecules in cell-like

structures formed by micelles. In certain cases, self-assembly can be driven by both entropy and enthalpy (Thomas et al., 2001)

Because self-assembly is an equilibrium process, the assembled components are in equilibrium with the individual components. The assembly (in practical circumstances there will be very many assemblies formed) is governed by the normal processes of nucleation and growth. Small assemblies are formed because of their increased lifetime as the attractive interactions between the components lower the Gibbs free energy, equation 2. As the assembly grows the Gibbs free energy continues to decrease until the assembly becomes stable for long periods. The necessity for this to be an equilibrium process is defined by the organisation of the structure which requires non-ideal arrangements to be sampled before the lowest energy configuration is found. If the process is to occur around room temperature the nature of the forces between the components must necessarily by quite small i.e. of the order of kT. Thus, the forces tend to be intermolecular in type rather than ionic or covalent which would 'lock' the assembly into non-equilibrium structures. The types of forces seen in most self-assembly processes are van der Waals, hydrogen bonds, weak polar forces, metal chelation, etc (Lindoy and Atkinson, 2001).

As regular structural arrangements are frequently observed (and, in fact, why many self-assembling processes find potential application in modern technologies) in self-assembly (although the formation of ordered structures is not necessary in a self-assembling system) it is clear that there must be a balance of attractive and repulsive forces between entities or else an equilibrium distance would not exist between the particles. The repulsive forces can be electron cloud – electron cloud overlap, electrostatic or derive from the differences in cohesive energies between the assembling components. Since, for practical reasons, the assembly is generally not at the atomic or small molecule scale (for practical reasons outlined below) it is generally necessary that both attractive and repulsive forces are long range interactions (as distinct from short range chemical bonds) if the separation distance between features is to be in the nanometre range. This can be illustrated using very simple consideration of the intermolecular forces between the entities. If we assume that the attractive intermolecular forces can be modelled as an attractive potential between similar point charges (Q), the potential energy (V_{att}) follows a 1/r dependence and can be written as:

$$V_{att} = -Q^2/4\pi\varepsilon_o r \tag{3}$$

where r is the separation of the entities. The repulsive charge can be modelled as $V_{rep} \alpha 1/r^n$. Assuming a charge of around 1.37×10^{-19} C and a repulsive constant = 10000 $(10^{-9})^n$ kJ mol^{-1} the variation in the total potential-distance curves ($V_{tot} = V_{att} + V_{rep}$) as a function of n in the repulsion term can be plotted, figure 1(A). The curves describe a classic potential energy well with a minimum V_{tot} at an equilibrium separation distance between the entities. It is worth noting since RT ~ 2.5 kJ mol^{-1}, that the minimum value of V_{tot} must be significantly greater than this to provide a driving force for assembly that compensates for an entropy decrease (equation 1). The minimum value of V_{tot} can be approximately associated with ΔH_{SA} assuming that there is no volume or temperature change during self-assembly. The attractive term is long range in nature and the width of the potential energy well that is formed is defined, in this case, the repulsive term. At n = 4 there is a well-defined potential energy minimum. This is important because it will precisely define an equilibrium distance between entities that is necessary if structural regularity is going to be high. The effect of increasing n, *i.e.*, increasing the short-range nature of the repulsive forces, is to reduce the value of the potential energy minimum, increase the width of the potential energy well and

move the minimum to greater distances. The increasing shallowness of the well is a major problem in terms of generating patterns of high structural regularity because it ensures a variation in spacing between entities (or features in phase-separated systems outlined below) can exist with little energy cost.

The effect of increasing the dependence of potential energy with distance, *i.e.*, increasing the short-range nature of the attractive potential, also has a dramatic effect on the potential energy curve. This is modelled using a V_{att} that follows a $1/r^n$ dependence whilst using a constant repulsive term that varies as $1/r^6$. Illustrative data are shown in Figure 1B. Increasing the value of n reduces the value of the potential energy minimum, increases the width of the potential energy well and moves the minimum to greater distances as described for the repulsive forces above. However, as n increases the decrease in the value of the potential energy minimum is very considerable such that changing n from 1 to 3 reduces the potential energy minimum by a factor of around ~x 150. Although these are quite simple calculations they do illustrate some important concepts in self-assembly on the mesoscale. Firstly, if the entities are to be relatively large distances apart, the repulsive and attractive forces between the entities will need to be relatively high or the potential energy will not provide an effective driving force at room temperature. Secondly, as the spacing between entities or features increases, variations in the separation distance within the self-assembled structure will increase dramatically and lead to poor structural regularity. Finally, for self-assembly to be effective, there needs to be a delicate balance of the intermolecular forces and because of this self-assembly with high structural regularity is not common-place and will require careful molecular or particle design coupled to optimisation of the process.

Finally, it should be stressed that self-assembly is a spontaneous chemical process where entities or components within a mixture arrange themselves in a structured manner and these processes take place in normal chemistry environments *e.g.*, solution mediated. Normally the self-organisation is borne from an initially disordered system. Importantly the equilibrium low-energy arrangement is reached from positional fluctuations as a result of thermal effects. Thus, the effective interaction potential between the entities or components cannot exceed thermal energy by too great a factor or else it will not be possible to minimise positional errors in the in the arrangement. Alternatively, there has to be enough difference between thermal energy and the interaction potential energy to maintain order within the pattern.

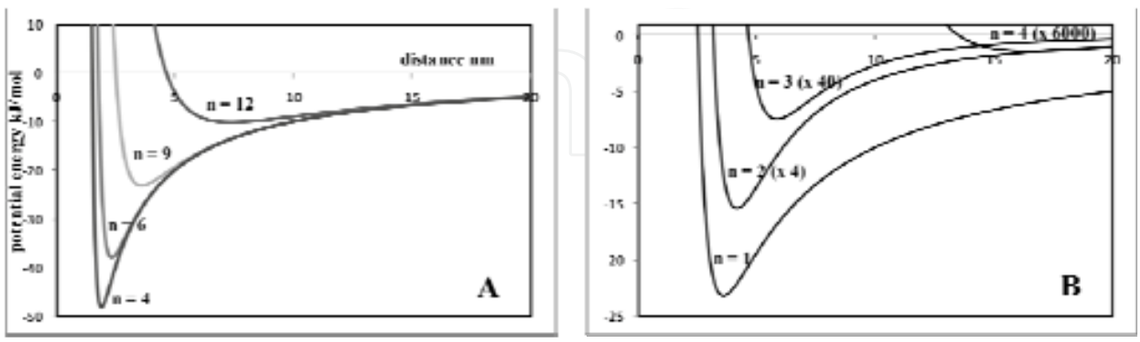

Fig. 1. Potential energy against distance curves. A – result of increasing the short range nature of the repulsive forces between entities in a self-assembly process. Note the increasing width of potential energy well. B – result of increasing the short range nature of the attractive forces between entities in a self assembly process. Note the dramatic decrease in the depth of the well.

1.2 The need for low defect concentrations in self-assembled systems

The self-assembly of BCP (block copolymer) systems can be more properly described as microphase separation and is becoming a subject of research for potential commercial development. Few self-assembling systems can approach the structural regularity of BCP systems, with perhaps only mesoporous silicates (Rice et al., 2007), track-etched polycarbonate membrane (Fang and Leddy, 1995) and porous anodic alumina (Petkov et al., 2007) rivalling the polymer systems in the feature size range of interest and having been shown to offer opportunities for controlled alignment. It can be seen from the arguments made above that the high regularity of the systems is because the intermolecular forces that drive the self-assembly are such that highly periodic structures are favoured and ordering can be attained at practical temperatures. One of the advantages of the BCP self-assembly methodology compared to the other forms mentioned (in the other cases the final structure is not reversible on application of temperature because the structure has been templated via components that have been subsequently removed or through techniques where chemical bonds are either made or destroyed) is that the film can be 'annealed' after their formation to improve the regularity of the self-assembled structures and this approach is described further below. Other self-assembled systems such as nanoparticle superlattices (Pileni, 2001) also produce highly regular and sometimes complex structures but transferring them to a macroscopic scale is difficult. In general, nanoparticle self-assembly development has been limited because the synthesis of size mono- dispersed particles is challenging for all but a few systems and thin films of these tend to lack thermal and mechanical robustness. Compared to other techniques, BCP systems offer a combination of experimental advantages; thin films can be formed from simple solutions, the resultant films are robust, the feature size is highly controllable using polymer engineering and the films are readily processed (*e.g.*, in pattern transfer where the polymer pattern is transferred to the surface by selective etch processes (Borah et al., 2011 and Farrell et al., 2010). Authors have demonstrated many applications for microphase separated BCP thin films. BCP micelle systems have found commercial use in applications such as drug delivery but these are not the focus of the work described here and the reader is directed to some excellent reviews (Lodge, 2003) Applications for BCP films in the general area of materials science include solid state battery electrolytes (Soo et al., 1999) and membrane separation technologies (Ulbricht, 2006). Park and co-workers have provided an extensive review of technologies that might be developed using BCP thin films and these are largely in the area of development of strategies to develop nanoscale electronics, magnetics and photonics. These ICT focussed technologies include low dielectric materials for electrical insulation and reduction of crosstalk, high density magnetic storage media and photonic band gap crystals. By far the most researched area for use of these materials is as potential alternatives to conventional mask-based photolithography for fabrication of nanoelectronic circuitry. Photo-lithography has been the cornerstone of the electronics industry since the advent of the first silicon devices (Pease & Chou, 2008). The photolithographic process has been continually developed to allow the size of devices to be decreased and the density of devices constantly increased so that individual transistor sizes have shrank from cm type sizes to around 50 nm. The trend in resolution enhancement was, for many years, achieved by reducing the dimensions of the mask patterns whilst simultaneously decreasing the wavelength of the radiation (light) (Bloomstein et al., 2006). Currently, techniques such as immersion technologies whereby a liquid (usually water) is placed directly between the

final lens and photoresist surface resulting in a resolution enhancement defined by the refractive index of the liquid have allowed device engineers to pattern transfer feature sizes (65 or 45 nm generation) that are actually less than the wavelength of light used (193 nm). Device performance is ultimately limited by the density of transistors on the chip and it is clear that patterning requirements will continue to the 32 nm node and beyond. Although photolithography can potentially be used to create sub-10 nm device structures for high volume manufacturing processes, it will necessitate the use of deep UV (13 nm) and x-ray sources and these are associated with high costs and materials implications for the masks and resists (ITRS roadmap, 2005).

For these reasons, self-assembly may have importance for transistor manufacture beyond the 22 nm node. The advantages of self-assembly over conventional and non-lithographic methods include: (i) the reduction of source costs, (ii) elimination of masks and photoresists, (iii) non-existence of proximity affects, (iv) the possibility of developing 3D patterning techniques, (v) absence of diffraction restrictions to resolution and (vi) can be used to pattern materials with precision placement techniques by availing of templating (*i.e.*, deposition of materials within the structure, known as graphoepitaxy) or a chemical pattern (alternating surface chemistries). The microphase separation of block copolymers is emerging as the most promising method of assembling highly ordered nanopatterns at dimensionalities and regularity approaching the future device dimension requirements. These requirements are extremely challenging for self-assembly and lithography alike and include sub-nm line edge roughness and sub-4 nm positioning (of a feature expressed from the overlay registry requirements) accuracy for the 16 nm technology node. The potential application of BCPs in this area has been extensively reported and reviewed (Jeong et al., 2008). These reviews also detail the methods by which the polymer nanopatterns can be processed into active components (*i.e.*, nanowires, nanodots of semiconducting, magnetic or conducting materials). If BCPs are to ever contribute to the development of devices with these types of dimensions then control and minimisation of defects is essential. In the remainder of this chapter we will explore the thermodynamics of defect formation in BCP thin films.

2. Block copolymer systems

In order to understand how defects form in BCP thin films, it is first important to understand the energetic of BCP self –assembly. BCPs have become increasingly more important materials as routine design and synthesis of these polymers has become practical. BCPs were first developed to essentially tune the properties of the macromolecule between that of the two blocks individually. The advantage of using a single macromolecule rather than a blend is that the macroscopic phase separation in mixtures cannot occur. However, the chemical mismatch does lead to microphase separation as described below. Industrial synthesis of BCPs was first demonstrated in the 1950s by scientists at BASF and ICI around the development of triblock systems of poly(ethylene oxide) and poly(propylene oxide) as a new class of synthetic surfactants. Amongst many applications these found widespread use not only as surfactants but also as anti-foaming agents, cosmetic materials and drug release materials (D'Errico, 2006). More recently they have found use as versatile 'templating agents' for the generation of ordered nanoporous silicates allowing precise control of pore diameters. Spandex was the

first BCP to be widely known because of its use in textiles (spandex is an anagram of expands) and was invented by the DuPont chemist J. Shivers. It became apparent that the possibility of forming macromolecules with blocks of differing chemical properties could yield materials where the interaction of the different blocks would ordain important physical properties. Many aspects of BCPs have been reviewed in depth (Hamely, 2004). This article will be restricted to discussion of the formation of nanopatterns of these materials in thin film form on substrates. The nanopatterns are essentially the result of the self-organisation *via* microphase separation of the BCP at the surface and not *via* micelle formation and related phenomena of the BCP in solution. The term microphase separation is used because it is the chemical dissimilarity of the blocks which drive the different blocks apart but complete phase separation is not possible because of the covalent bonds linking the blocks. These bonds act as a restoring force and result in a series of ordered patterns as discussed below. Lyotropic phases will not be discussed at length here, however, solvent effects cannot be completely ignored because it is convenient and practical (particularly for the thin films discussed here) that the polymers are solvent cast onto the substrate surface by techniques such as dip- and spin-coating. Further, a technique known as solvent-annealing or solvent-swelling is becoming common place as a means of attaining high degrees of structural regularity. This ordering is a result of the increased mobility within the macromolecule block network related to the decrease in the glass transition temperature as a result of solvent molecule inclusion (Kim & Libera, 1998).

2.1 The thermodynamics of microphase separation in block copolymers

The thermodynamics of microphase separation in BCPs has been reviewed several times following the original work of Bates (Bates, 1991). The theory will not be detailed in depth here except to show how it relates to intermolecular forces through the solubility parameter and how the thermodynamics of defect formation in these systems can be properly understood. Most of the understanding of microphase separation of BCPs is centred on a term known as the interaction parameter χ. Assuming a simple di-block copolymer made up of sub-units A and B, the χ value resulting from the interactions between block A and block B can be written as:

$$\chi = z\Delta w/kT \tag{4}$$

and χ is the exchange energy per molecule normalised by the thermal energy kT and is dimensionless. The number of neighbours surrounding one block is z. Δw is the exchange energy which is the difference in energy between the interaction between block A and block B and the average of the self interactions between block A-block A and block B-block B. That is, Δw is the energy cost of taking a block of A from surrounding A blocks and placing in a B block environment and doing the same for a B block (from a B environment to an A environment). The interaction parameter can be related directly to the molar enthalpy change of mixing, ΔH_m, by:

$$\Delta H_m = f_A f_B \chi RT \tag{5}$$

where f_A and f_B are the volume fractions of the blocks. By conventional solution theory and assuming no volume change on mixing, it can be shown that:

$$\chi = V_m(\delta_A - \delta_B)^2/RT \tag{6}$$

where δ_A and δ_B are the solvent parameters (see below) of the two blocks. Therefore:

$$\Delta H_m = f_A f_B V_m(\delta_A - \delta_B)^2 \quad (7)$$

This is important because it shows that any block copolymer system where the blocks have different solubility parameters (*i.e.*, different strengths and forms of intermolecular interactions) will have a positive enthalpy of mixing and will, thus, have a tendency to microphase separate and self-assemble provided the entropy change (which in the case of BCP self-assembly always decreases as discussed above) associated with the process is not too large as to overcome the enthalpy contribution. Flory-Huggins theory has been the basis for modelling the behaviour of block copolymers since their invention and remains the most used model to date providing a robust basis for the prediction of morphology seen in BCP microphase separated systems. Using this formulism the configurational entropy of phase separation is assumed as the only major contribution to energy such that the entropy associated with microphase separation $\Delta S_m = k\ln\Omega$ where Ω is the number of possible ways of arranging the system. *Via* Stirling's approximation the entropy change can be written as can be written as:

$$\Delta S_m/RT = (1/N_A)\ln f_A + (1/N_B)\ln f_B \quad (8)$$

where N_A, N_B are the degrees of polymerisation of each block such that $f_A = N_A/(N_A + N_B)$. Since the entropy decreases in the system on mixing and using equation 5:

$$\Delta G_m/RT = f_A f_B \chi + (1/N_A)\ln f_A + (1/N_B)\ln f_B \quad (9)$$

This Equation specifically relates to the mixing process and not phase separation. The implication is that the free energy of mixing is always likely to be positive bearing in mind the definition of χ given in equations 4 and 6. The driving force for self-assembly is the minimisation of the free energy of mixing by the regular patterns formed by microphase separation. For illustrative purposes consider the formation of a regular, microphase separated, lamellar phase consisting of alternating stripes of blocks from a AB block copolymer with $f_A = f_B$. The lamellar structure is a common motif in phase separation because it is achieved with lowest mass transport limitations. This is particularly important considering that phase separation is limited by the covalent bonding between blocks and all theories suggest this is the lowest energy structure for BCPs. As can be seen from equation 4, ordered self-assembly/microphase separation will occur provided that $\Delta G_{SA} = G_{mix} - G_{PS}$ is negative. The free energy change in forming the lamellar structure ($\Delta G_{SA,L}$) can be described by modelling G_{mix} as a sum of AB contacts and G_{PS} as a Hookian term describing the balance of repulsive enthalpic and attractive/restorative entropic forces (as detailed above) plus an interfacial term. In this way (Matsen & Bates, 1996) the G_{PS} can be written:

$$G_{PS} = 1.19(\chi_{AB}N)^{1/3} \quad (10)$$

and the equilibrium spacing between stripes in the lamellar structure (L) as:

$$L = 1.03a(\chi AB)1/^6N^{2/3} \quad (11)$$

Since the sum of simple contacts in the mixed system allows G_{mix} to be estimated as $(\chi_{AB}N)/4$ it is possible to write that for microphase separation to occur G_{mix} must be greater or equal to G_{PS} and the minimum condition is:

$$1.19(\chi_{AB}N)^{1/3} = (\chi_{AB}N)/4 \quad (12)$$

Thus, for microphase separation $\chi_{AB}N$ must be greater than 10.4. Since χ_{AB} is a measure of the chemical dissimilarity between the units (mers) in the blocks $\chi_{AB}N$ represents the total dissimilarity over the whole macromolecule. Using equation 12 the minimum value of $(\chi_{AB}N)_{min}$ to bring about phase separation is about 10.4. This very simple approach provides a value for $(\chi_{AB}N)_{min}$ which is very similar to much more complex theories developed by Leibler using self-consistent field theory (Leibler, 1980). A summary of recent theoretical developments in block copolymer phase separation has been provided by Grason (Grason, 2006).

3. Origin of defects

In a self-assembled structure there are likely to be reasonable concentrations of defects. This is suggested in equation 1, $\Delta G_{SA} = \Delta H_{SA} - T\Delta S_{SA,}$ because in most cases the thermodynamic driving force for self-assembly is provided by weak intermolecular interactions and is usually of the same order of magnitude as the entropy term. Practically, for any self-assembling system to reach the minimum free energy configuration there must be enough thermal energy to allow the mass transport of the self-assembling moieties. In these circumstances, obtaining defect free self-assembly over macroscopic areas is improbable. A self-assembled nanopatterned surface is likely to show a number of distinct irregularities or defects and these can take many forms as outlined below. The origins of these defects are manifold but each defect comes with an energy cost because it disrupts the arrangement of the polymer blocks which provides a free energy minimum within the film.

3.1 Equilibrium defects

As above, the thermodynamically defined concentration of defects originates from a balance of configurational entropy and the energy cost associated with the defect. These defects are 'statistical' in nature and while individual defects may have limited lifetimes a population of them will always exist at a concentration defined by conditions. The thermodynamics of defects in fully equilibrated systems is well understood but care must be taken to separate the free energy defining self-assembly and pattern formation from the free energy of defect formation so that the role of intermolecular forces can be well understood. For defect formation the free energy of single defect formation is given by:

$$\Delta G_{DF} = \Delta H_{DF} - T\Delta S_{DF} \quad (13)$$

The enthalpy term, ΔH_{DF}, does not necessarily reflect the intermolecular forces between blocks – it is the energy cost associated with disrupting the pattern and may be thought of as a region where optimum arrangement does not occur and the reduction of enthalpy associated with ideal self-assembly is not realised. For example, a system of hexagonally packed cylinders may exhibit defect regions of lamellar structure. The enthalpy of defect formation is partially related to the enthalpic difference between the two structural arrangements and this might be much less than the intermolecular forces between blocks. If the difference in enthalpy of two different arrangements is small a relatively high equilibrium concentration of defects might be expected compared to one where the enthalpy difference is large. The entropy difference now reflects the order change between the prefect and defective structural arrangement. Note here that the enthalpy cost of creating a defect is

not only determined by the respective differences in structural arrangement but also by strain energy (due to tensile and compressive forces that are associated with defect insertion) as well as any interfacial effects arising from intermolecular interactions in the areas around the defect . If ΔG_{DF} is negative there will be a finite number of defects in the system and the concentration will be given by:

$$N/N_0 = \exp(-\Delta E_{act}/RT) \tag{14}$$

N is the number of defects in a matrix of N_0 self-assembled moieties or features and ΔE_{act} is the activation energy of defect formation. The activation energy ΔE_{act} should not be confused with ΔH_{DF}. The activation energy represents energy difference between the initial ideally arranged state and a transition state towards the defective structure. Equation 13 can be used to estimate the defect concentration by use of the Boltzmann formula to estimate entropy S

$$S = k\ln W \tag{15}$$

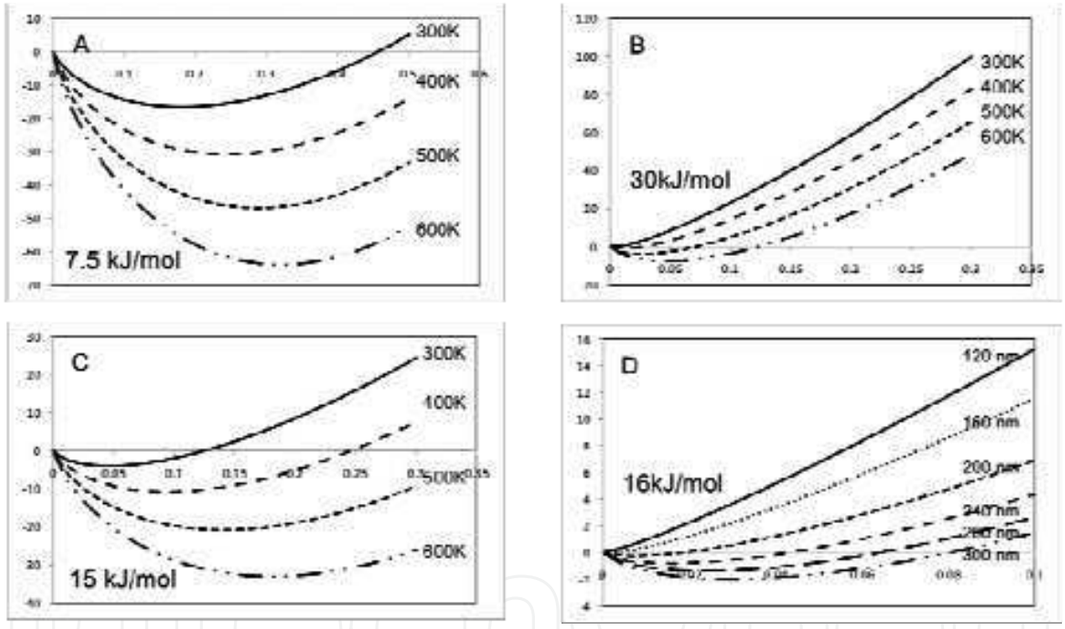

Fig. 2. (A) – (C) Free energy of defect formation as a function of defect concentration (as ratio of defects to total number of features) for three different activation energies for defect formation. (D) Free energy of defect formation versus defect concentration at various channel widths.

where W is the number of ways of arranging n defects over N possible features within a system of periodic structure. W can be written:

$$W = N!/((N-n)!n!) \tag{16}$$

and using Stirling's approximation we can write that :

$$\ln N! \sim N \ln N - N \tag{17}$$

so that:

$$T\Delta S_{DF} = kT[N \ln N - n \ln n - (N - n) \ln (N-n)] \quad (18)$$

and:

$$\Delta G_{DF(n)} = n\Delta H_{DF} - kT[N \ln N - n \ln n - (N - n) \ln (N-n)] \quad (19)$$

where $\Delta G_{DF(n)}$ represents the free energy cost of forming n defects in the system. This formulism allows a plot of free energy against n/N, the defect ratio, as shown in Figure 3. Three plots (Figures 3A-C) are shown for three different defect formation energies typical of what might be expected for a BCP system *e.g.*, Hammond (Hammond et al., 2008) has measured the defect formation energy in a PS-*b*-P2VP system at around 30 kJ mol^{-1}. Although these are simple calculations they illustrate the salient features of equilibrium defect formation.

At low defect concentrations defect formation is entropy driven until a critical concentration of defects allows the activation energy term to compensate for entropy. There is usually an equilibrium defect density indicated at the minimum free energy. As might be expected, as the activation energy for defect formation increases this equilibrium defect density. At high activation energy values (*e.g.*, around 30 kJ mol^{-1}) and low temperature (300 K) there is no thermodynamic driving force for defect formation and the data suggests that in BCP systems it should be possible to form highly regular structures.

3.2 Non-equilibrium defects

Practically, there are few examples of defect free microphase separation of BCP thin film systems even in cases where the number of equilibrium defects is vanishingly small. As these films are normally prepared by non-equilibrium methods such as spin- or dip-coating the microphase separated structure evolves by either thermal or solvent annealing and defects are introduced (nucleation of microphase separated regions) or removed by growth kinetics. Through the annealing cycle phase separated regions will nucleate in various places, grow and increase in order (Segalman et al., 2003). This growth will produce the classical structural motif of a 'polycrystalline' type grain structure where local ideal arrangements are separated from one another by extended defects akin to grain boundaries. Grains will grow by consumption of smaller grains and this process will be kinetically limited as described below. Other non-equilibrium or extrinsic defects can be present and these include defects induced by surface flaws, poor polymer size dispersion and impurity inclusion.

Theoretically, non-equilibrium defects resulting from pattern errors (as distinct from those precipitated by surface defects, impurities etc.) can be removed by annealing; providing enough thermal energy to allow ideal configurations to be sampled thereby increasing the size of the regions of the ideal arrangement. However, due to the nature of the chemical interactions between blocks (which can be rather small) and the relatively high glass transition temperatures (which limit polymer chain mobility needed to sample the ideal ordered arrangement) coupled to low meting points and low order-disorder temperatures, the temperature window for annealing out these non-equilibrium defects may be rather small and the defects may be essentially kinetically metastable. In many examples in the literature, BCP films are ordered at just above the glass transition temperature conferring enough chain mobility but as far as practically possible from the order-disorder

temperature. This methodology may necessitate very extended heating times to remove defects and practically (because of local and large area mass transport limitations) equilibrium may not be achieved even after inordinately long annealing periods and non-equilibrium defects will still be present. This is largely due to the requirement for defect annihilation associated with coarsening of the randomly orientated grain structure described above that results from the kinetics of nucleation and growth of phase separated regions (Harrison et al., 2000). Thus, although ΔG_{DF} may be positive for many BCP systems, implying no defects should be formed if the system attains complete equilibrium, in practice this is unlikely. In many cases a clear distinction of equilibrium defects and non-equilibrium defects cannot be practically achieved. The advent of advanced force microscopy methods facilitates defect studies without causing damage to the sample. Of particular importance are *in situ* AFM methods that allow real time data collection during pattern evolution.

3.3 Experimental studies of defect reduction in block copolymer systems

The defects that can occur in BCP nanopatterns can take several forms and it is beyond the scope of this chapter to detail these in full, however, it is worth providing a general overview. They take the form of many structural defects in other systems and can be broadly described as dislocations and disclinations and a good review is provided elsewhere (Krohner and Antony, 1975). In the simplest explanation, a dislocation is a defect that affects the positional order of atoms in a lattice and the displacement of atoms from their ideal positions is a symmetry of the medium. Screw and edge dislocations representing insertion of planes or lines of atoms are typical of dislocations. For a disclination the defects (lines, planes or 3D shapes) the rotational symmetry is altered through displacements that do not comply with the symmetry of the environment. Kleman and Friedel give an excellent review of the application of these topics to modern materials science (Kleman and Friedel, 2008).

A number of di-block BCP patterns (more complex BCPS are beyond the scope of this article) exist as a function of composition and temperature and these have been fully described elsewhere (Morris et al., 2009).The two most important phases from an application point are a lamellar phase (at a composition of around 50:50) and a hexagonal phase (composition around 33:66). The lamellar phase exists as sheets of each block arranged in a stripe pattern. A typical example is shown in figure 3. Lamellar structures can be seen in figure 3 (A and B). Normally, they adopt a 'fingerprint pattern' with a complex series of swirls and regions of parallel lines as shown in figure 3 (A) for the diblock BCP polystyrene–b–polymethylmethacrylate (PS–b–PMMA with a molecular weight of around 18,000 g mol^{-1} for each block) . The lamellae (sheets that form stripes) can be vertical to the surface plane as shown or horizontal depending on the surface chemistry. They adopt this complex fingerprint structure because this structure, since the sheets are largely parallel even though they do curve, allows almost complete minimization of the intermolecular force derived enthalpy factors driving self-assembly. However, entropy is increased and the pattern therefore allows minimisation of free energy. In certain cases where the structure can be directed (i.e. self-assembly) by interaction with pre-patterned chemistries known as chemical patterning (Nealey, 2000). The pre-patterns have a preferred chemistry with one block (e.g. hydrophobic – hydrophobic) that constrains the BCP pattern to the underlying chemical pattern. Another form of directed self-assembly is using surface topography to confer preferential pattern alignment to, e.g., the sidewall within a trench or similar. This is

known as graphoepitaxy and is detailed further below. An example of the same BCP used in figure 3 (A) that has been directed into a more regular structure is shown in figure 3 (B). In this case the pattern was directed by surface strain. Figure 3 (C and D) shows patterns for a PS–b–PMMA BCP of block molecular weights around 42,000 and 21,000 g mol^{-1} respectively. This is a cylinder forming system where PMMA cylinders are distributed in an hexagonal arrangement through a PS matrix. The orientation of the cylinders, i.e. parallel or vertical to the surface plane, is determined by the surface chemistry (Hawker et al., 1997). Surfaces that are neutral, i.e. they interact with both blocks to a similar extent will cause vertical orientation of the pattern so that the PMMA cylinders are vertical to the surface plane as shown in figure 3 (C). If the surface chemically favours the matrix block, PS in this example, the cylinders will be parallel to the surface plane as shown in figure 3 (D). This arrangement forms fingerprint patterns similar to those exhibited by the lamellar structure and it can be difficult to distinguish these phases by top-down imaging alone. Surface chemistry manipulation is of great concern in controlling polymer patterns and in other forms of self-assembly.

Also shown in figure 3 are some typical pattern defects. In figure 3 (A) the circle marks an area that encloses an edge dislocation and an extra 'line' has been inserted into the pattern. The boxes in the same image mark areas enclosing disclinations which are very common in this 'fingerprint' structure. In figure 3 (C) the box marks what can be described as a ground boundary separating two distinct alignments of the hexagonal pattern. This sort of grain boundary is made up of a number of dislocations and disclinations. As discussed above, these defects may originate from equilibrium or non-equilibrium effects although absolute assignment can be difficult. The majority of dislocations and disclinations are probably equilibrium in nature but may also arise from imperfections imposed by surface flaws and impurities. Grain boundaries may similarly be of both types. Other types of defects can exist. Mis-orientation is common particularly if the substrate surface chemistry is not isotropic and variation in height etc can occur unless coating procedures and surface chemistry are very carefully controlled (Fitzgerald et al., 2009)

The thermodynamic and kinetic limitations of forming ideal self-assembled patterns are clear. In many self-assembled systems such as mesoporous silicates any defects are frozen in during synthesis because the self-assembled structure acts as a template for the formation of the final ordered structure. In this case an ordered micellar arrangement is a framework around which an inorganic framework condenses. As mentioned above, one of the key advantages of the BCP microphase separation self-assembly is the ability to anneal and reduce defect densities towards their equilibrium value. Optimum annealing temperatures have generally not been determined and are likely to vary as a function of composition and molecular weight of the BCP (since these determine the magnitude of the glass transition and melting temperature). Choice of annealing temperatures is not simple. The optimum temperature is one where ordering is achieved in a practical time but is low enough to reduce the equilibrium defect concentration to a level demanded by the application for which the materials will be used. Cooling rates are important because films may reach an equilibrium at elevated containing more equilibrium defects than desirable (but thereby allow high concentrations of extrinsic to be annealed out) but cooling at an appropriate rate would allow the equilibrium concentration to be reduced. Cooling too quickly will effectively 'freeze-in' a non-equilibrium defect concentration. The sensitivity of BCP microphase separation to temperature in thin films is illustrated below. This also shows some of the essential elements of this self-assembly mechanism.

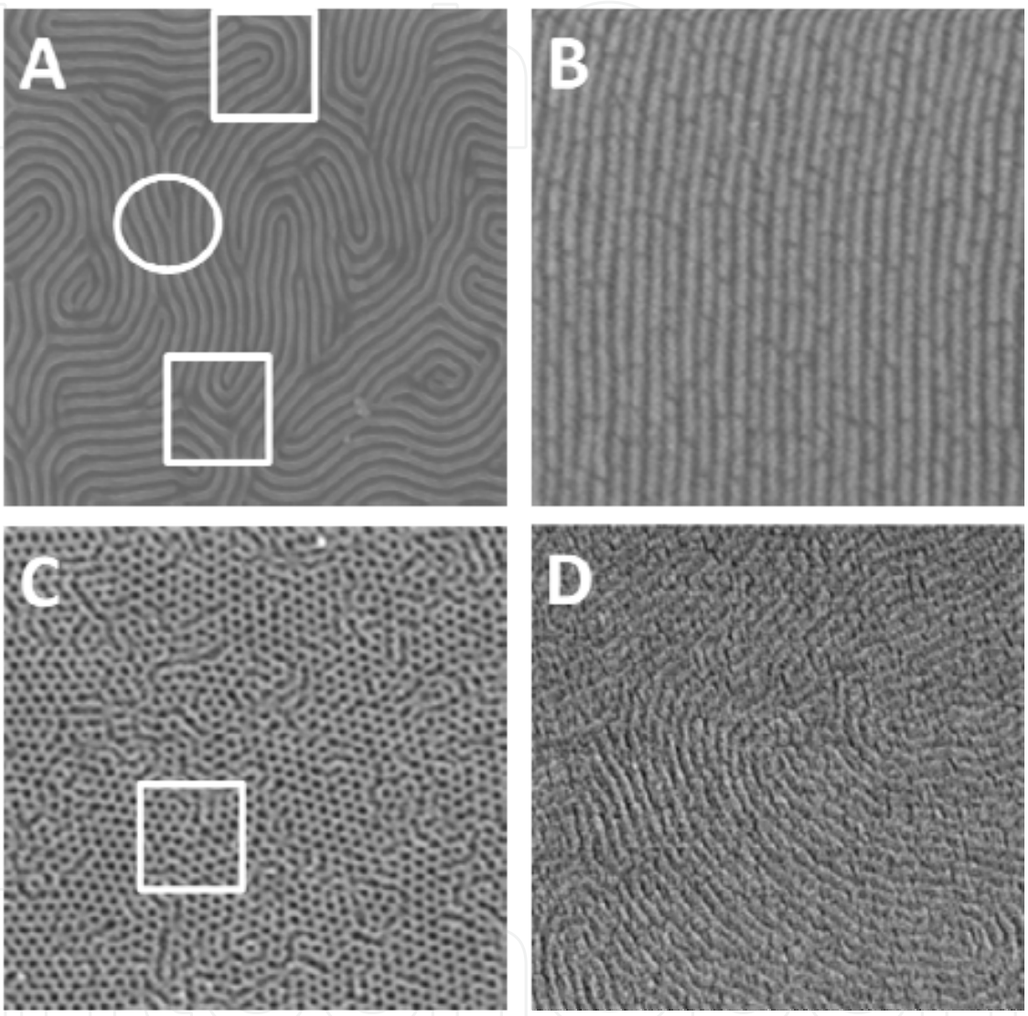

Fig. 3. Typical PS–b–PMMA BCP patterns formed via microphase separation. (A) and (B) are representations of a lamellar self-assembly (18,000–18,000 g mol^{-1} BCP composition). (C) and (D) are representations of a hexagonal arrangement from a PS–b–PMMA BCP of composition 42,000 and 21,000 g mol^{-1} respectively. Areas marked are described in the text. Images shown are representations of 1 μm x 1 μm (upper images) and 4 μm x 4 μm (lower images). Images were taken by secondary electron microscopy after selective removal of the PMMA block.

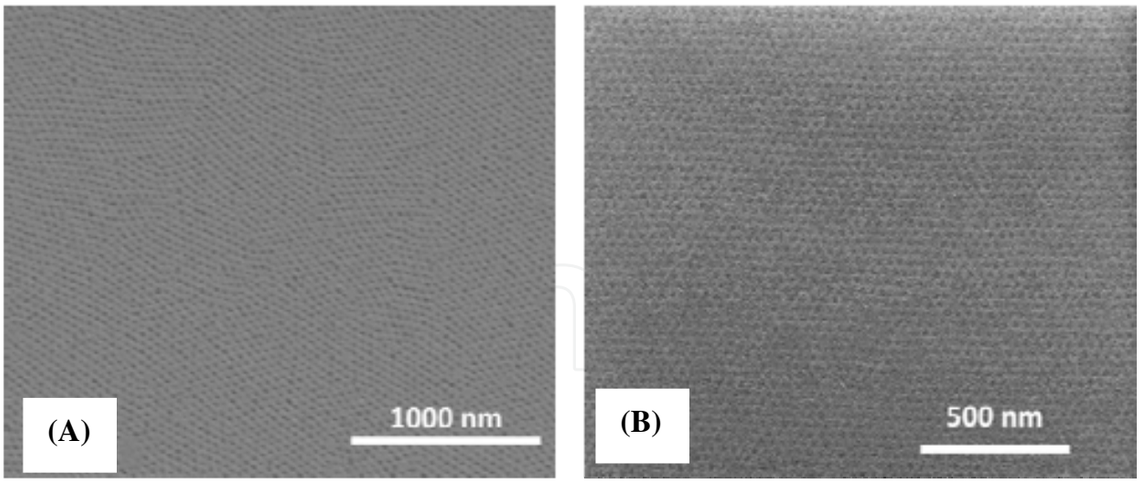

Fig. 4. PS-b-PEO thin films on silicon substrates. (A) PS-b-PEO of molecular weight 42,000–11,500 g mol^{-1} and (B) PS-b-PEO of molecular weight 32,000–11,000 g mol^{-1}. Images were taken by secondary electron microscopy after selective removal of the PEO block. It is relatively easy (in the left hand image) to see grain boundary type structures as the areas where one alignment of the structure exist are quite large.

The polymers used in figure 4 were polystyrene–polyethylene oxide (PS-b-PEO) block copolymer but of differing molecular weights. Each film was cast to be around 50 nm thick and the composition is such is to form a regular hexagonal arrangement of PEO cylinders in a PS matrix. Good microphase separation in each was achieved by identical solvent annealing in a mixture of toluene/water. Solvent annealing is an alternative to simple annealing where a solvent atmosphere allows the polymer to swell (toluene swells PS and water PEO). During swelling, the glass transition temperature decreases because the polymer chains are separated by the solvent molecules allowing low temperature treatments to bring about annealing [Fitzgerald et al. 2009). Although the molecular weights are quite similar, the difference in long-range order between the two polymers is remarkable. For the higher molecular weight the polymer has a classic grain-type structure where regions of a well-ordered hexagonal phase are separated by boundaries between different rotations. For the lower molecular weight, the entire image is a single grain with no grain-boundaries present (note that this terminology is used loosely as this is not a true grain boundary in the strictest sense since this is not a crystalline structure). The difference in the degree of long-range order probably results from the lower molecular weight having a lower glass transition temperature and hence having greater chain mobility. In this polymer, the structural changes are probably occurring during cooling because it has been shown that fast cooling rates can produce re-orientation of the cylinders in the film form this vertical alignment (i.e. cylinders normal to the surface plane) to cylinders parallel to the surface plane. This represents an important point in many cases of self-assembly. Even though the self-assembled organisations are formed at or close to equilibrium, they are often removed from the equilibrium conditions for further processing and characterisation. Examples of this include: solvent evaporation, cooling, pressure reduction, dehydration and chemical reactions and their effects.

As mentioned above, these BCP films have the advantage that they can be progressively improved by annealing to reach an equilibrium condition where the number of defects can be minimised. Many other forms of self-assembly are processes where the structure is a

representation of the minimum free energy configuration in the presence of a solvent. E.g. in the assembly of nanoparticles, the particles are brought together to the arrangement of lowest free energy via diffusion within a solvent. When the solvent is removed to produce a film for example, the structure cannot readily be refined because of the rigidity of the product. BCP thin films are normally cast from solution (either spin-coated or dip-coated usually) and solvent is removed to produce a non-equilibrium structure. Frequently, this structure may be partly microphase separated but it is unusual for regular arrangements to be achieved during processing of the film because solvent evaporation rates are fast. Microphase separation is then promoted through an ageing (if chain movement is rapid enough around room temperature) or annealing step. During annealing (or ageing) the film will move towards the equilibrium structure at that temperature before being cooled for use or characterisation. The final structure may represent the equilibrium structure at the annealing temperature, the temperature it is reduced to or an intermediate temperature depending on the cooling rate.

Of course, during annealing, the copolymer system will move towards equilibrium with the concentration of defects given by a Boltzmann type distribution function, i.e. as shown in equation 15. However, it may be practically impossible to achieve the equilibrium as there are severe mass transport limitations to the movement of the polymer chains. Dis-entanglement requires many coherent chain movements and there will be considerable kinetic barriers to achieving equilibrium which is a structure of a single domain extending across the substrate.

Since, the microphase separated block copolymer arrangement can be nucleated at many sites across the substrate (as discussed above) the progress towards the equilibrium structure can be viewed as a type of grain coarsening akin to that seen in metallurgy. In this way, non-equilibrium defect structures formed after coating consist of poly grain structures whose size can be extended by lengthening of the anneal time and annihilation of the defects. As outlined below, the growth of domains is kinetically limited and the process slow. Grain growth in these systems has been shown to follow a $t^{0.25}$ power law (Harrison et al., 2000). If this law is generally obeyed then a plot of the number of defects against $1/t^4$ should be straight line with an intercept on the y-axis of the equilibrium number of defects. Note, however, characterising the number of defects at elevated temperature is experimentally difficult to quantify and caution must be applied in studies of this type. Atomic force microscopy (AFM) and secondary electron microscopy (SEM) are usually used to observe these patterns but are difficult techniques at high temperatures particularly when significant pressures of solvent. Thus, the number of defects resulting from an annealing step is observed at room temperature in conditions well removed from the annealing process. Thus, as explained above, the actual number of defects may not represent an equilibrium value at the annealing temperature.

Typical kinetic studies are shown in figures 3 to 6 three BCP systems showing hexagonal arrangements of the minority phase in a matrix of the major phases. These polymers were polystyrene-polyethylene oxide (PS-*b*-PEO, 32,000–11,000 g mol^{-1}) polystyrene-polymethylmethacrylate (PS-*b*-PMMA, 42,000-21,000 g mol^{-1}) and polystyrene-polyferrocenyl dimethylsilane (PS-*b*-PFS, 60,000-30,000 g mol^{-1}). The samples were cast onto standard cleaned silicon (100) substrates and then annealed. As cast films are generally very poorly ordered as shown by typical AFMs in figure 4. Annealing brings about considerable improvement in the film patterns as shown in figures 5-7. It should be noted that for the PS-b-PMMA film that both pattern defects and film defects are present. The film defects

originate from poor wetting of the silicon surface by the BCP. However, in all cases the pattern defects do show a linear decrease with 1/anneal time^4 in agreement with the general model. In all cases, the number of defects is visually counted with a 2 μm x 2 μm image. In all cases, the plot of number of defects versus time show that the defect annihilation rate is very slow at extended times. In no case shown is the number of defects at equilibrium equal to zero as indicated by the intercept in the linearised form of the data. This is an important point in the study of self-assembly; the self-assembled pattern is likely to have a considerable number of defects present regardless of the care taken in synthesis or preparation. The potential use of self-assembly as a nanofabrication tool has been limited by the fact that they cannot rival techniques such as photolithography where defect concentrations close to zero can be engineered.

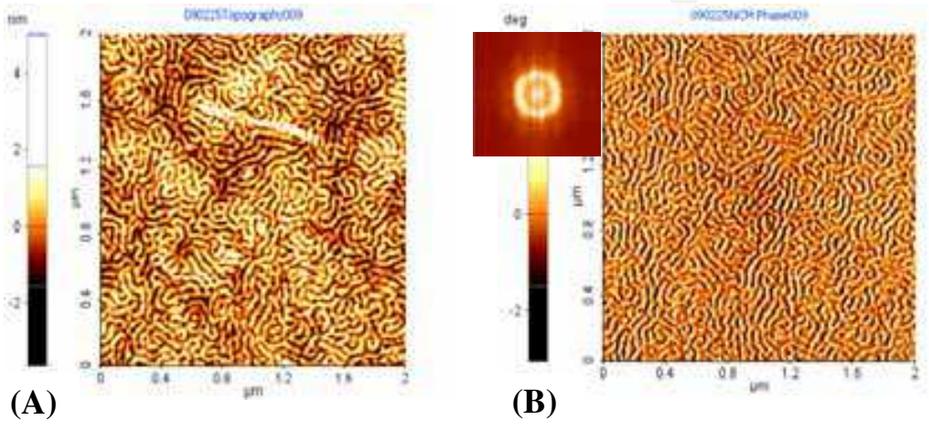

Fig. 5. AFM topography (A) and phase (B) images of PS-*b*-PFS thin films prepared from 1.0 wt% solution of polymer in toluene prior to any annealing. Some limited short-range order is present as indicated by the Fourier transform data shown as an insert in (A).

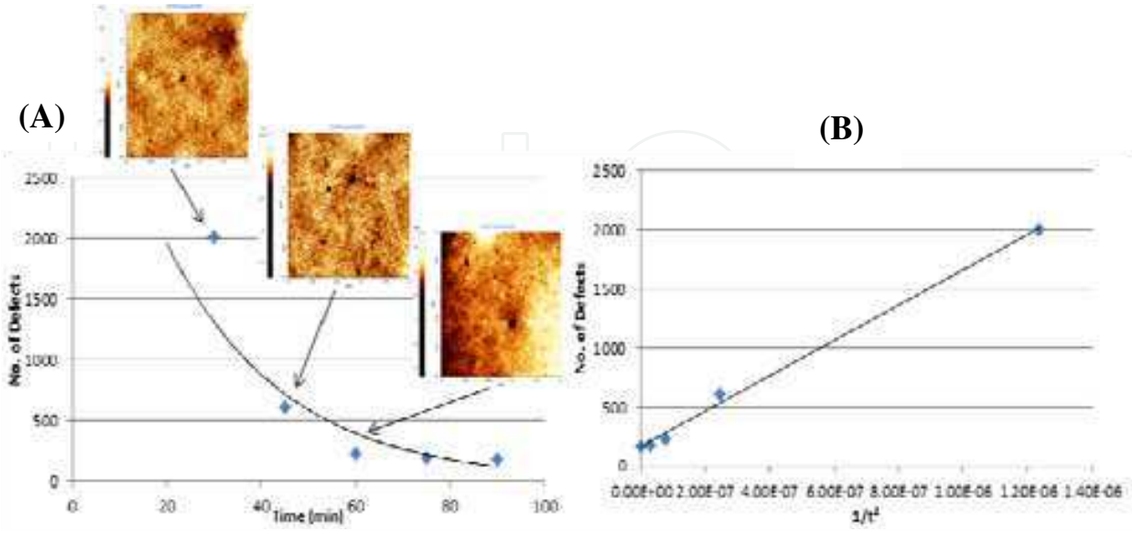

Fig. 5. Graphs plotting (A) the no. of defects vs. anneal time and (B) no. of defects vs. 1/t^4 (where t is the anneal time) of PS-b-PEO thin films (solvent annealed in a toluene/water atmosphere at 50^{0}C for various times)

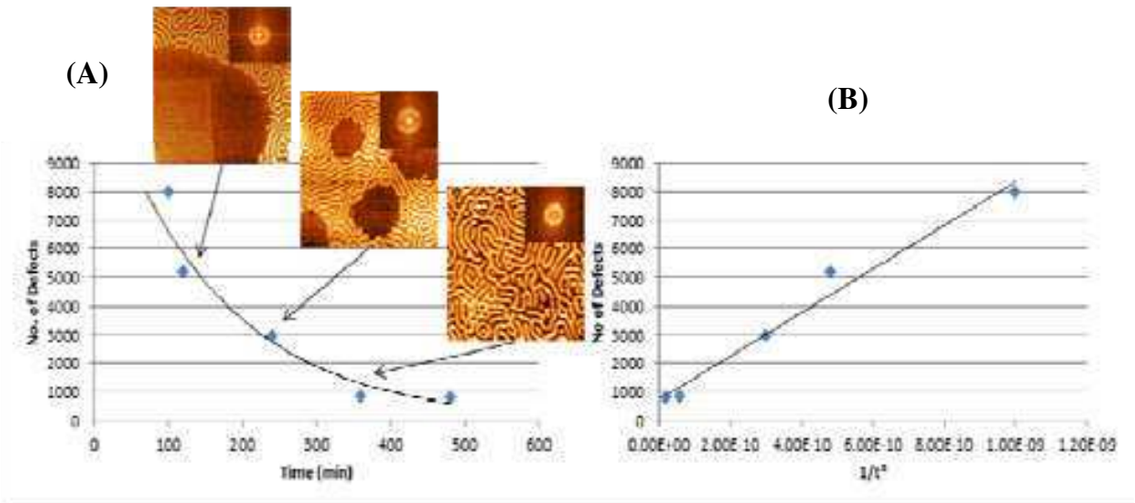

Fig. 6. Graphs plotting (A) the no. of defects vs. anneal time and (B) no. of defects vs. $1/t^4$ (where t is the anneal time) of PS-b-PMMA thin films (thermal annealed at 170^0C for various times)

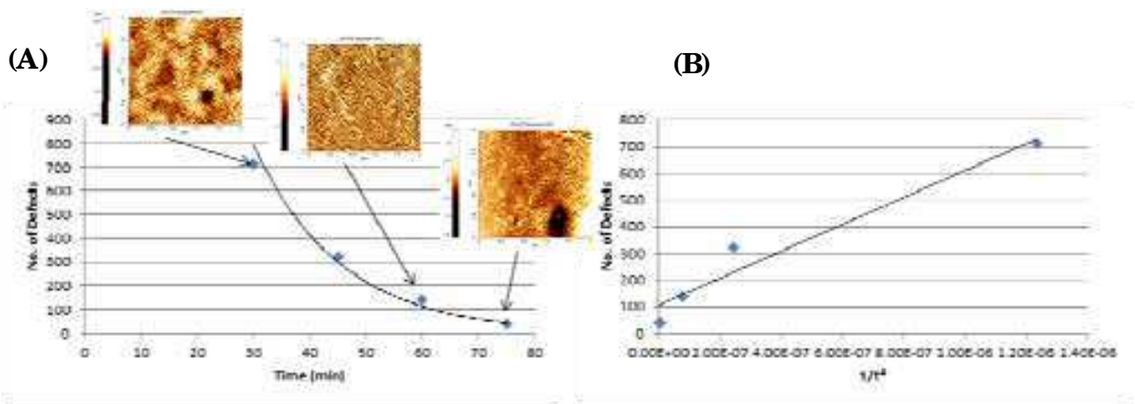

Fig. 7. Graphs plotting (A) the no. of defects vs. anneal time and (B) no. of defects vs. $1/t^4$ (where t is the anneal time) of PS-b-PFS thin films (solvent annealed in a THF atmosphere at room temperature for various times)

4. Graphoepitaxy

As was briefly mentioned above, one method used to reduce defect concentration and control alignment is graphoepitaxy. Graphoepitaxy is where surface topography is used to direct the BCP structure. The term graphoepitaxy was originally coined to describe how a substrate topographic periodicity can be used to control the crystallographic alignment of thin films and the technique evolved to become a popular method for defining highly crystalline polymer films. It is generally accepted that strain imposed by the topography is the origin of the alignment effects; however, chemical interactions of the BCP with the topography (as outlined below) probably play a more significant role in influencing the alignment process. As discussed further in the following sections, it will be seen how by engineering the preferential interaction of one block with the topography can ordain pattern alignment eliminating the

fingerprint patterns described above. Of equal importance is the reduction in defect density within these aligned patterns that is also provided by the topography. This seems to derive from a number of factors. Firstly, the strong polymer-sidewall interactions that increase the enthalpic driving force for regular assembly. Secondly, and associated with this enthalpic effect is the increased energy cost of including defects which are also associated with localisation of higher strain energies around the defect. Finally, there is the spatial constraint of the pattern which makes inclusion of defects statistically less likely.

The advantage of graphoepitaxial techniques for BCP nanopattern development is that a single relatively large substrate feature such as a channel can be used to direct the BCP nanopattern with precise alignment into almost single crystal-like periodicity within the topographically defined feature. Fasolka et al. (Fasolka et al., 1997) were the first researchers to show that corrugated substrate surfaces could be used to direct the development of microphase separated block copolymers. These authors used a simple off-cut silicon substrate to generate a sawtooth topography and this was sufficient to generate regular BCP periodicity. Segalman was the first author to demonstrate that designer topography (in this work channels or rectangular cross-section separated by flat terraces or mesas and examples provided here will refer only to this shape) could be used to generate aligned, to the edge of the channel, nanopatterns of extremely high periodicity (Segalman et al., 2001). Segalaman's ground-breaking work not only demonstrated the possibility of this methodology for control of BCP structures but also reported the possibility of unusual edge effects due to varying film thickness as well as proposing a mechanism for alignment. It was suggested that alignment occurs *via* nucleation at the channel walls and that, below a critical channel width, a single domain structure could be formed.

Graphoepitaxy represents a means to combine established methods of surface engineering such as uv-lithography (to generate topography) and chemical functionalisation (to define the interaction of the BCP with the topography formed) to impose alignment on the walls. Chemical functionalisation, as mentioned above, is critical and a recent paper by Nealey et al. (Nealey et al., 2010) described how polymer brushes can be used to fine-tune the polymer-topography interactions. A polymer brush is a random co-polymer of the two blocks used in the self-assembling BCP. Changing the composition of the random brush allows the interactions to be modified. Efforts to control the polymer-topography interactions have led to the development of a technique known as soft-graphoepitaxy where the topography is generated from polymer materials (usually lithographic resist materials) that allow specific interactions with one block. The surface engineering must also be carefully controlled. If simple rectangular, cross-section channels are used the width of the channels should be a simple geometric ratio to the spacing of the pattern allowing for preferential wetting of one block at the sidewall or else defects will be precipitated as discussed below. Practically, this can be difficult to achieve and Nealey et al. have shown how the use of mixtures of the BCP with homopolymers can be used to modify the feature size of the BCP pattern to match the surface topography.

Segalman's original work on BCP graphoepitaxy was based around aligned sphere forming polystyrene-*b*-poly(2-vinylpyridine) (PS-*b*-PVP) di-block copolymers. The work has progressed very quickly and reached a high level of sophistication (see for example the review by Segalman et al.). Work reported to date has demonstrated alignment of both horizontal and vertical orientations of cylinder forming systems and sphere forming systems. One area of considerable importance has been the development 'sparse' surface topographies which minimise the size of the topographical features and considerably reduce

the mesa contribution. Ross and co-workers have developed this technique to align vertical cylinders or spheres so that a low density of 'posts' guide the structure whilst being almost indistinguishable in terms of position, size and chemistry from a feature in the BCP nanopatterns (Bita et al., 2008). These sphere and vertical cylinder structures can be used to create column or nanodot structures by pattern transfer or templating methods.

In terms of emerging electronic structures or interconnect arrangements, the formation of parallel nanowires at a substrate has become an important challenge. So-called FIN-FET structures consisting of several nanowires controlled through a single gate has become an important topic of research because it may provide an alternative form of transistor to the well-established metal oxide semiconductor structure at very small transistor sizes. There has, therefore, been considerable work on the controlled alignment of lamellar (stripes orientated vertically to surface plane, Figure 3B) and cylinder (parallel to surface plane, Figure 3D) forming BCPs where coupling these techniques with templating (selective deposition into the structure) and/or pattern transfer (where the pattern is selectively etched chemically or physically can transform these structures into nanowire arrays. PS-*b*-PMMA is of particular interest because of the well-established etch characteristics of this system and has been shown to successfully produce transistor-type device structures (Black et al., 2007). The development of ultra-small circuitry (not only devices but also interconnects, vias, magnetics and capacitors has provided the motivation of much of the work into both graphoepitaxy and chemical patterning briefly described here. This is because, in practical and useful structures, it is not only necessary to define an arrangement, but also accurately position the structures so that wiring can be overlaid to define their function.

It is also emphasised that forming well-aligned and positioned parallel (to the surface plane) arrangements of BCPs offers some further challenges compared to vertical cylinder arrangements e.g. Film thickness and transfer of polymer to the channels can present a number of experimental difficulties. Suh et al. studied orientation effects in cylinder forming block copolymer films in detail and it is now generally accepted that vertical orientation of the cylinders is favoured for very thin films because the parallel arrangement can only be sustained with inclusion of elastic strain in the structure at low dimension (this strain effectively reduces with thickness). The reason for this can be viewed thermodynamically because there will always be a finite difference in the free energy of a parallel and vertical structure because of interactions with the substrate modifying the enthalpy of the pattern. If e.g. the film is below a thickness where a whole number of layers can be formed in a parallel arrangement of cylinders, the film must either deform to allow an integer number or layers or allow the formation of incomplete layers which increases surface roughness. Both of these effects are associated with increased surface strain and reduction of the total free energy. Although this strain is effectively reduced with layer thickness (spread over a larger volume of the BCP), it is extremely important to control the orientation in the cylinder forming patterns because only single layers of cylinders are required if the pattern is to be used for creation of devices since multilayer structures cannot be readily filled or transferred to the substrate by etch or template methods. The importance of controlling film thickness within graphoepitaxial channels has been recently discussed in detail (Fitzgerald, 2009)

4.1 Defects and graphoepitaxy

It should be immediately apparent that graphoepitaxy will have a profound effect on defect formation. Ideally, topography-polymer interactions and topographical dimensions will be such to allow the BCP to form a 'perfect' structure (i.e. with an equilibrium number of

defects only). Confining the polymer to distinct and small regions of a substrate should also decrease kinetic limitations defined by mass transport over large substrate surfaces. This may also have significant practical implications because, as can be seen above in figures 5-7, many hours are needed to produce well-ordered arrangements and such long periods may not be compatible with commercial manufacturing processes.

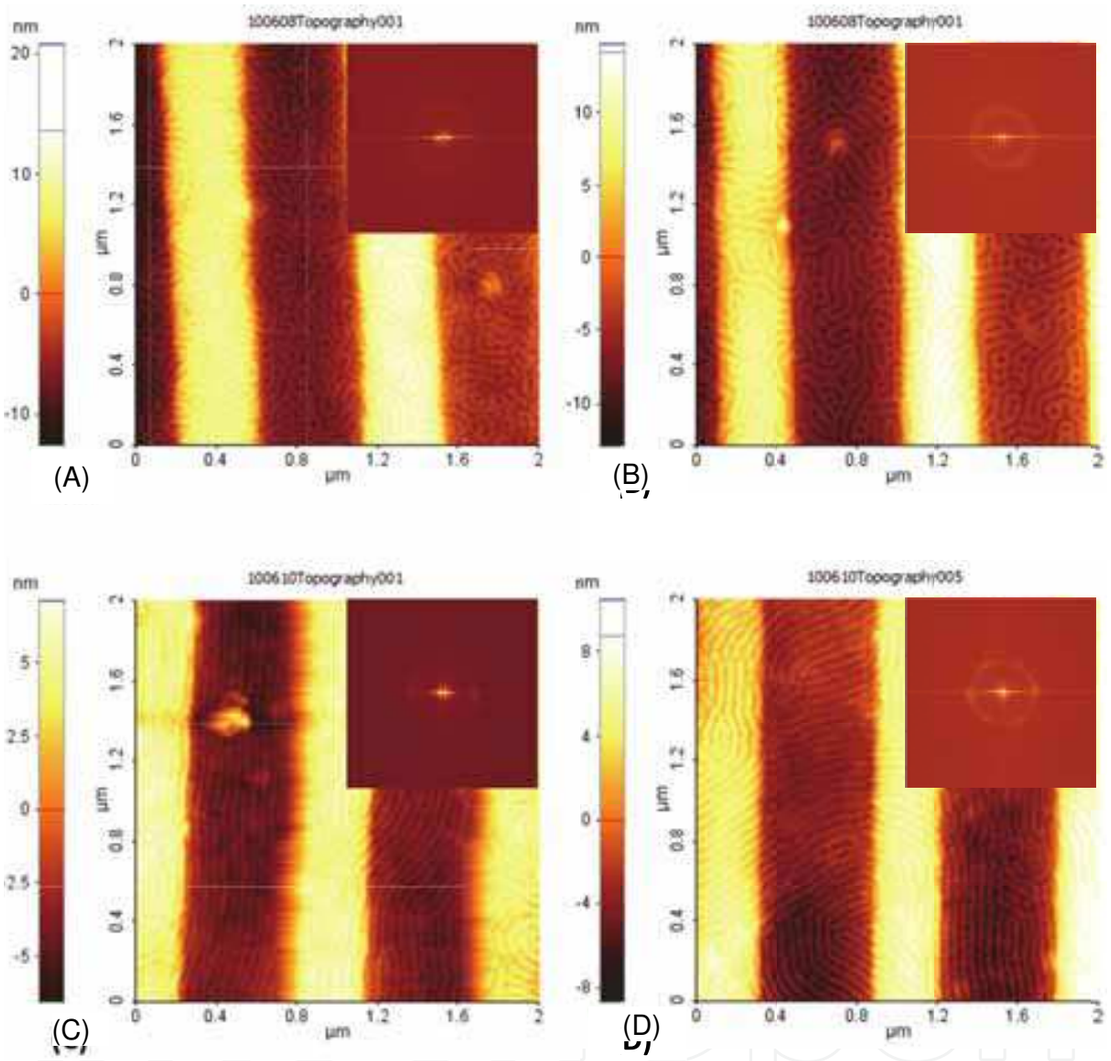

Fig. 8. AFM topographic images of PS-PFS thin films prepared from 0.5 wt% solutions of polymer in toluene on channel cut topographically defined substrates (600 nm channels) after solvent annealing in THF at room temperature for (A) 0 min, (B) 15 min, (C) 30 min, (D) 60 min

Some recent data from our laboratories (figure 8) show the importance of the relationship between the anneal time and alignment/defect numbers in topographical substrates and the necessity to control the placement of the polymer very carefully. The cylinder forming PS-b-PFS (60000-30000 g mol^{-1}) system on Si(100) substrates has a strong tendency to form parallel arrangements of cylinders. We assert that this is because chemical interactions with both the substrate and the surface interface strongly favour PS wetting layers and vertical

arrangements where the PFS component contacts the substrate are not thermodynamically favourable. If this pattern forming BCP is spun-cast onto channel cut topographically defined substrates (600 nm channels), this results in a non-uniform film adopting the corrugation of the substrate where polymer is located on the top of the crests (or mesas) as well as within the channels as can be clearly seen from patterns over the entire surface. At this point the film is highly disordered and exhibits a random dispersion of PFS domains in the PS matrix (figure 8A). Solvent annealing in a THF-dominant atmosphere allows chain mobility and after 15 min there is an increase in the level of ordering though there is no directional effects from the sidewalls identified (figure 8B). It should be noted this level of ordering is significantly greater than seen in figure 7C because of the constraint of the polymer and reduction in kinetic limitations described above. Further annealing periods can lead to the eventual formation of a well-ordered parallel arrangement of cylinders (figure 8C and D). The alignment of the pattern to the sidewalls is not ideal over the entire surface because it is not possible to locate polymer only in the trenches and where the BCP covers the mesas, a more random orientation can occur (figure 8D) as the cylinders are able to escape the constraining effects of the channels. However, it is important to note that alignment and orientation is nucleated at the channel edge (figure 8C) and can be passed into the mesa structures. Presumably this is because of the favourable interactions of the PS component with the side wall.

Whilst it is highly unlikely that a true minimum energy configuration of a BCP film on a flat substrate (i.e. only an equilibrium number of defects present) can be achieved over a large area flat substrate because of all the effects outlined above, in confined systems it may be possible to achieve close to this minimum energy arrangement in highly localised regions of topography if film coating can be suitably controlled. In these cases (and if the pattern can be aligned to a substrate feature through favourable chemical interactions) then random grain orientations can be avoided and the requirement for defect annihilation during grain coarsening via very long period anneals can be decreased or essentially eliminated. Thus, close to ideally ordered arrangements may be achieved. Graphoepitaxy as described above, therefore, offer a means of aligning patterns and thus potentially provide a solution to problems associated with forming defect free films for manufacturing purposes. It, thus, seems necessary that these bottom-up techniques for patterned surface formation are combined with a top-down lithographic method in order to achieve ideal arrangements. One innovative approach to the problem of developing and use of advanced lithography is to use the assembly of another block copolymer film which can be readily aligned through favourable interactions with substrate features (see below). This polymer film is then subsequently used to chemically pattern the BCP of interest. This approach has been used with a cylinder forming PS-*b*-PMMA system to form a chemical pattern for development of well-ordered lamellar forming PS-*b*-PMMA (Black et al, 2007).

Low defect concentrations in BCP phase separated structures have been reported using graphoepitaxial methods. As discussed above, in favourable circumstances the topographically patterned surfaces align and orientate the phase separated BCP structure through interactions between the surfaces and one or both blocks. These interactions force the BCP structure into registry and single grain structures. There are many examples in the literature of graphoepitaxial defined single grain structures (Fitzgerald et al., 2007). Various authors report that the defect nature of these directed structures are largely insensitive to the match between polymer feature spacing and channel width (commensurability) except that as width increases there is a corresponding increase in the number of polymer features within the topography. It is of course noted, as outlined above, that the polymer structure

will exhibit strain (*i.e.*, the spacing between features will stretch or compress) so as to fit an integer number of features across the topography such that strain is minimised. As shown by Ross and co-workers (Ross et al., 2004) the energy of the system will be minimum at the trench width at which commensurability occurs (*i.e.*, width = n polymer feature spacings, n = an integer) but will increase at higher or lower values. The strain energy will be at a maximum when the trench width is equivalent to n + ½ polymer feature spacings).

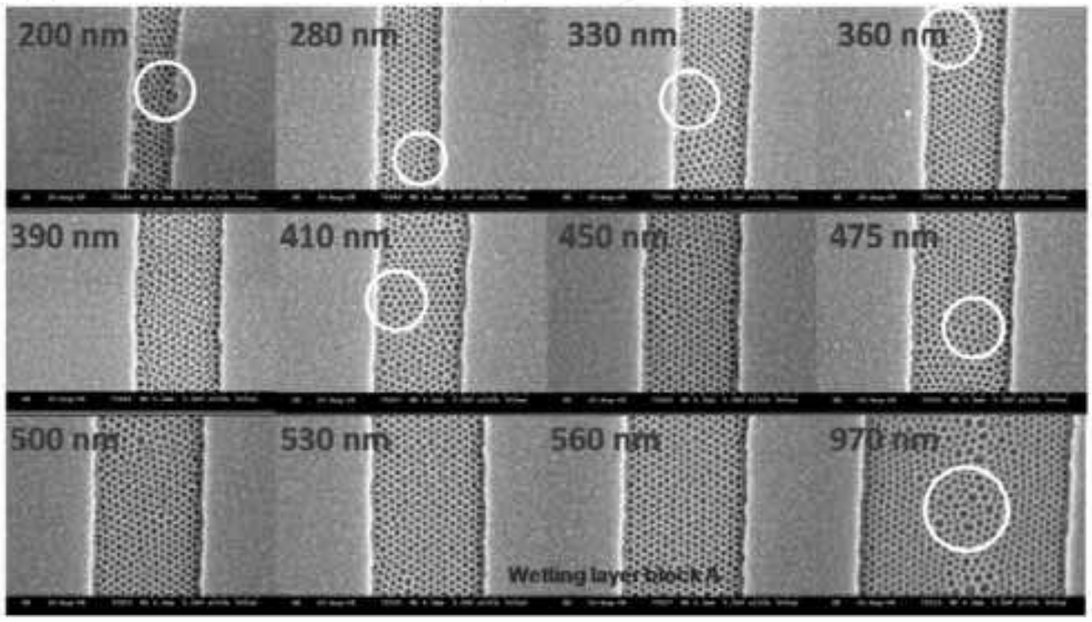

Fig. 9. SEM images of etched cylinder forming PS-b-PEO (PEO removed) in rectangular trenches (60 nm depth and width as shown) of various widths. The white circles show various defects present including grain boundaries, dislocations and point defects. See text for further details.

Some of the data from these laboratories illustrates some of the important defect chemistry of BCP systems in topographical patterns when studying the cylinder forming PS-*b*-PEO system. These data are summarised as in figure 9 and shows the patterns formed as a function of width of a channel generated in Si(100) wafers by uv-lithography. In this data, great care was taken to use polymer amounts that just provided enough material to fill the channels. In all cases, defect free, single grain structures were a rarity and clear grain boundary type and other types of defect structures can be seen with some marked for convenience (white circles). There is an obvious reduction in defect density at channel widths of 390 and 560 nm and we suggest that these values are commensurate with the pattern feature size as discussed above. Analysis of the data in figure 9 suggests a number of other points. Firstly, the sidewall structure is not ideal and can be readily seen around narrower trench widths. These cause a local variation in channel width that is of the same order of magnitude as the polymer pattern feature size. This variation must by necessity introduce high local strain energies and consequently causes the precipitation of defects and, thus, defect concentrations are relatively high. As the width increases the defect concentration observed apparently decreases until at very high widths it increases again. We explain these observations in the following manner. The BCP energy is dominated by block-block and block-interface interactions so that filling of the topography and maximising the

number of features within the topography are the most important factors. When the channel width and phase separated feature spacing is incommensurate, strain energy (highly dependent on the polymer properties) results and an ideal pattern can only be achieved if this strain energy is less than the total energy recoverable from changes in structure and defect formation. Thus, as width increases it becomes easier to maintain ideal single grain, defect free structures because the strain is distributed over a larger polymer volume and so is proportionally less. At very large channel widths nucleation can occur at both side walls leaving an area at centre where defects must form to allow volume fill.

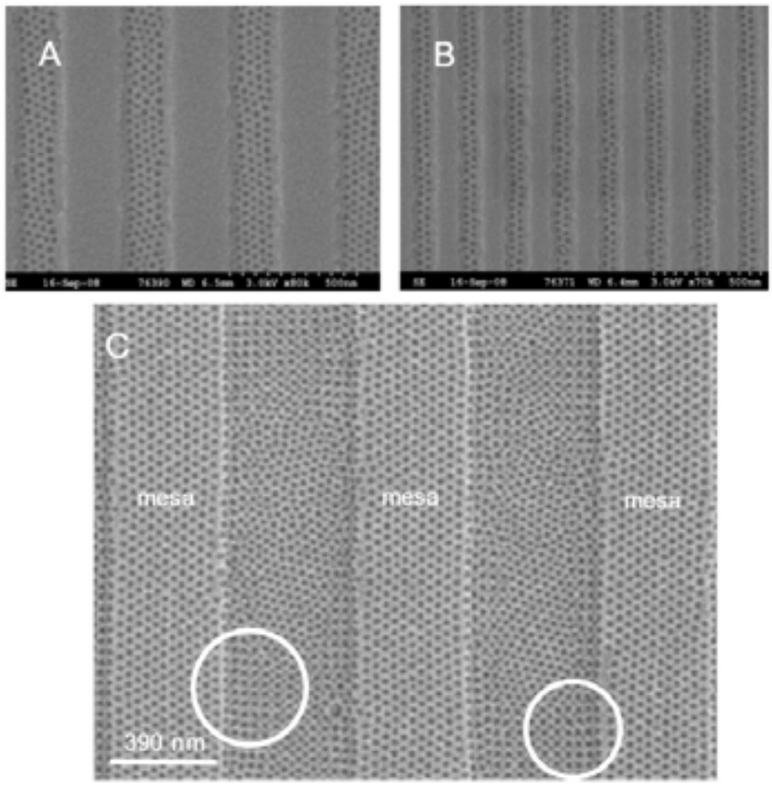

Fig. 10. SEM images of etched cylinder forming PS-b-PEO (PEO removed) in rectangular trenches (60 nm depth and widths of 175 (A), 120 (B) and 390 (C) nm). Polymer was deposited to just fill channels in (A) and (B) but was overfileld in (C) to allow phase separation at the mesas.

If this description is correct there should be a minimum channel width where no equilibrium defects should be observed since the introduction of strain energy would raise the total energy of the system excessively. This can be modelled in the same way as described above in figure 2 except that the activation energy for defect formation (a value of 16 kJ mol^{-1} was used) is effectively increased by an incommensurate strain energy of 4 kJ mol^{-1}. It was further assumed that this incommensurate strain was dispersed over the volume of polymer in the channel. The results are shown in Figure 2(D) which illustrates that even when defect formation is favourable, that there is a critical dimension when there should be no equilibrium defects formed. Figure 10 provides experimental support for this model. In the narrowest channel widths of 20 nm, there is an almost ideal arrangement of BCP structure. Figure 10(C) provides clear evidence that the majority of defects observed in graphoepitaxy result from the strain

introduced by the channels. Here, a cylinder forming PS-*b*-PEO polymer was spin-coated to create material at the channel mesas and within the channel. The BCP structure within the channel is highly defective with the defect motifs seen above clearly visible. Also the expected hexagonal pattern is not exhibited uniformly and an unexpected cubic arrangement of the cylinders is observed in places as a result of the imposed strain. This cubic pattern clearly has a feature spacing that is commensurate with the channel width. However, at the mesas, an almost ideal structure is seen. This can be explained by the fact that any strain caused by incommensurity can be relieved by a slight expansion of the film.

5. Conclusions

The microphase separation of block copolymers shows a great deal of promise as a means of generating regular nanopatterns at surfaces. They may, therefore, find application as a means to novel nanomaterials and nanoelectronics device structures. The possible formation of these patterns is thermodynamically determined by the strength of the chemical interactions which is balanced by entropy considerations. Polymer composition determines the structural arrangement whilst molecular weight and the physical properties determine the kinetics of the phase separation process. However, in thin film form the chemical interactions between the blocks and their environment, *i.e.*, the interfaces that surround them, must also be carefully considered so that the microphase structure exhibits controlled alignment and orientation. The use of surface engineering to control the chemical interactions with the surface and chemical pre-patterning are strict needs if the requirements for long-range order and periodicity are to be met. Like all self-assembly processes, defect concentration is of vital important and these systems can exhibit a number of defects originating from thermodynamic and kinetic limitations. Recent work, as featured above, suggests that defect-free patterns over macroscopic dimensions may be achievable. However, a much more detailed understanding of the origin of such defects will be required before processes that reduce defect concentration to the number required by the microelectronics industry can be put in place.

6. Acknowledgements

We would thank SFI though funding via the CRANN CSET scheme as well as for funding Prof. Morris and Dr. Holmes under the Principal Investigator Scheme. The authors would like to acknowledge the EU FP7 programme for funding the LAMAND consortium under the NMP scheme and in particular for support of Dr. O'Mahony. The authors would like to thank Intel Ireland and Intel Components Research for provision and development of patterned silicon wafers under the Adaptive Grid Substrate CRANN programme. Staff at the CRANN Advanced Microscopy Laboratories and Central Equipment Facility as well as staff at The Tyndall National Institute are thanked for their expertise and access to facilities.

7. References

Whitesides, G.M.; Grzybowski, B. Self-assembly at all scales. *Science* 2002, *295*, 2418-2421.

Whitesides, G.M.; Mathias, J.P.; Seto, C.T. Molecular self-assembly and nanochemistry: A chemical strategy for the synthesis of nanostructures. *Science* 1991, *254*, 1312-1319

Misteli, T. The concept of self-organization in cellular architecture. *J Cell Biol.* 2001, *155*, 181–185.
Jones, R.L., *Soft Machines*, Oxford University Press, Oxford, New-York, 2004.
Bensaude-Vincent, B., Self-Assembly, Self-Organization: Nanotechnology and Vitalism. *Nanoethics* 2009, *3(1)*, 31-42.
Grzybowski B. A., Wilmer, C. E., Kim, J., Browne, K. P. and Bishop, K. J. M., *Soft Matter*, 2009, *5*, 1110-1128.
Halley, J. D. and Winkler, D. A., *Complexity*, 2008, *14*, 10-17.
Gerhart, J. and Kirschner, M., Embryos and Evolution, *Blackwell Science*, MA, USA, 1997.
Nicolas, G. and Prigogine, I., Self-Organization in Non-Equilibrium Systems, *Weinheim*, New York, USA, 1995.
Capone, B., Pierleoni, C., Hansen, J-P. and Krakoviack, V., *J Phys. Chem. B*, 2009, *113 (12)*, 3629–3638.
Adams, M., Dogic, Z., Keller, S. L. and Fraden, S., *Nature*, 1998, *393*, 349-352.
Fraden, S., Maret, G., Caspar, D.L.D and Meyer, R. B., *Phys. Rev. Lett.*, 1989, *63*, 2068-2071.
Bai, G., Wang, Y., Yan, H., Li, Z. and Thomas, R.K., *JColloid Interface Science*, 2001, *240*, 375-377.
Lindoy, L.F. and Atkinson, I.M., Self-Assembly in supramolecular systems, *The Royal Society of Chemistry*, Cambridge, UK, 2001.
Rice, R.; Arnold, D.C.; Shaw, M.T.; Lacopina, I.; Quinn, A.J.; Amenitsch, H.; Holmes, J.D.; Morris, M.A. Ordered mesoporous silicate structures as potential templates for nanowire growth. *Adv. Funct. Mater*. 2007, *17*, 133-141.
Fang, Y. and Leddy, J., *J Phys. Chem.*, 1995, *99*, 6064.
Petkov, N.; Platschek, B.; Morris, M.A.; Holmes, J.D.; Bein, T. Oriented growth of metal and semiconductor nanostructures within aligned mesoporous channels. *Chem. Mater*. 2007, *19*, 1376-1381.
Pileni, M.P. Nanocrystal Self-Assemblies: Fabrication and Collective Properties. *J Phys. Chem.* B 2001, *105*, 3358–3371.
Borah, D., Shaw, M.T., Rasappa, S., Farrell, R.A., O'Mahony, C., Faulkner, C.M., Bosea, M., Gleeson, P., Holmes, J.D. and Morris, M.A., J. Phys. D: Appl. Phys., 2011, *44*, 174012.
Farrell, R.A., Petkov, N., Shaw, M.T., Djara, V., Holmes, J.D. and Morris. M.A., Macromolecules, 2010, *43 (20)*, 8651–8655.
Lodge, T.P. Block Copolymers: Past Successes and Future Challenges. *Macromol. Chem. Phys*. 2003, *204*, 265-273.
Soo, P.P.; Huang, B.Y.; Jang, Y.I.; Chiang, Y.M.; Sadoway, D.R.; Mayes, A.M. Rubbery block copolymer electrolytes. *J Electrochem. Soc*. 1999, *146*, 32-37.
Ulbricht, M. Advanced functional polymer membranes. *Polymer* 2006, *47*, 2217-2262.
Pease, R.F.; Chou, S.Y. Lithography and other patterning techniques for future electronics. *Pro. IEEE*. 2008, *96*, 248-270.
Bloomstein, T.M.; Marchant, M.F.; Deneault, S.; Hardy, D.E.; Rothschild, M. 22-nm immersion interference lithography. *Opt. Express* 2006, *14*, 6434-6443.
ITRS roadmap 2005 [Online.] Available: http://www.itrs.net/.
Jeong, S.J.; Xia, G.; Kim, B.H.; Shin, D.O.; Kwon, S.H.; Kang, S.W.; Kim, O.S. Universal block copolymer lithography for metals, semiconductors, ceramics, and polymers. *Adv. Mater*. 2008, *20*, 1898-1904.
D'Errico, G. In *Encyclopaedia of Surface and Colloid Science*, Somasundaran P., Ed.; CRC Press: Boca Raton, FL, USA, 2006; p. 3840-3848.

Hamley, I.W. *Developments in Block Copolymer Science and Technology*; Wiley: Hoboken, New Jersey, 2004.

Kim, G.; Libera, M. Microstructural development in solvent-cast polystyrene-polybutadiene-polystyrene (SBS) triblock copolymer thin films. *Macromolecules* 1998, *31*, 2569-2577.

Bates, F.S. Polymer-polymer phase behaviour. *Science* 1991, *251*, 898-905.

Matsen, M.W.; Bates, F.S. Unifying weak- and strong-segregation block copolymer theories. *Macromolecules*. 1996, *28*, 1091-1098.

Leibler, L. Theory of microphase separation in block copolymers. *Macromolecules* 1980, *13*, 1602-1617.

Grason, G.M. The Packing of Soft Materials: Molecular Asymmetry, Geometric Frustration and Optimal Lattices in Block Copolymer Melts. *Phys. Rep.* 2006, *433*, 1-64.

Hammond, M.R.; Cochran, E.; Fredrickson, G.H.; Kramer, E.J. Temperature dependence of order, disorder, and defects in laterally confined di-block copolymer cylinder monolayers. *Macromolecules* 2005, *38*, 6575-6585.

Segalman, R.A.; Hexemer, A.; Kramer, E.J. Edge effects on the order and freezing of a 2D Array of block copolymer spheres. *Phys. Rev. Letts*. 2003, 91, 196101/1-4.

Harrison, C.; Angelescu, D.E.; Trawick, M.; Zhengdong, C.; Huse, D.A.; Chaikin, P.M.; Vega, D.A.; Sebastian, J.M.; Register, R.A.; Adamson, D.H. Pattern coarsening in a 2D hexagonal system. *Europhys. Lett*. 2004, *67*, 800-806.

Kröner, E. and Anthony, K-H., *Annual Review of Material Science*, 1975, *5*, 43-72.

Kleman, M. and Fridel, J., *Reviews of Modern Physics*, 2008, *80* 61-115.

Farrell, R.A., Fitzgerald, T.G., Borah, D., Holmes, J.D. and Morris M.A., *J Mol. Sci.*, 2009, *10*, 3671-3712.

Peters, R.D., Yang, X.M., Wang, Q., de Pablo, J.J. and Nealey, P.F. *J Vac. Sci. Tech. B*, 2000, *18*, 3530-3534.

Mansky, P., Liu, Y., Huang, E., Russell, T.P. and Hawker, C.J., Controlling polymer-surface interactions with random copolymer brushes. *Science*, 1997, *275*, 1458-1460.

Fitzgerald, T.G., Farrell R.A., Petkov, N., Bolger, C.T., Shaw, M.T., Charpin, J.P.F, Gleeson, J.P., Holmes, J.D. and Morris M.A., *Langmuir*, 2009, *25*, 13551.

Fasolka, M.J.; Harris, D.J.; Mayes, A.M.; Yoon, M.; Mochrie, S.G.J. Observed substrate topography-mediated lateral patterning of di-block copolymer films. *Phys. Rev. Lett*. 1997, *79*, 3018-3021.

Bita, I.; Yang, J.K.W.; Jung, Y.S.; Ross, C.A.; Thomas, E.L .; Berggren, K.K Graphoepitaxy of self-assembled block copolymers on two-dimensional periodic patterned templates. *Science* 2008, *321*, 939-943.

Black, C.T.; Ruiz, Z.; Bretya, G.; Cheng, J.Y.; Colburn, M.E.; Guarini, K.W.; Kim, H.C .; Zhang, Y. Polymer self assembly in semiconductor microelectronics. *IBM J Res. Dev*. 2007, *51*, 605-633.

Fitzgerald, T.G.; Borsetto, F.; O'Callaghan, J.M.; Kosmala, B.; Shaw, M.T.; Holmes, J.D.; Morris, M.A. Polymer nanostructures in sub-micron lithographically defined channels: film-thickness effects on structural alignment of a small feature size polystyrene-polyisoprene-polystyrene block copolymer. *Soft Matter*. 2007, *2*, 916-921.

Cheng, J.Y.; Mayes, A.M.; Ross, C.A. Nanostructure engineering by templated self-assembly of block copolymers. *Nat. Mater*. 2004, *3*, 823-828.

Han, E., Kang, H., Liu, C-C., Nealey, P.F. and Gopalan, P., *Advanced Materials*, 2010, *22*, 4325-4329.

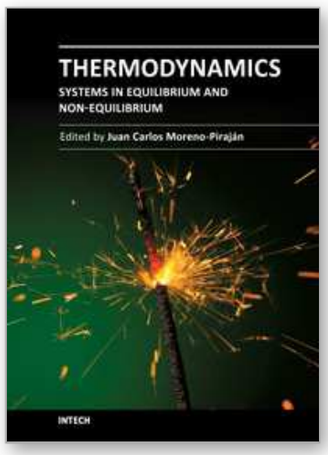

Thermodynamics - Systems in Equilibrium and Non-Equilibrium
Edited by Dr. Juan Carlos Moreno PirajÃ¡n

ISBN 978-953-307-283-8
Hard cover, 306 pages
Publisher InTech
Published online 10, October, 2011
Published in print edition October, 2011

Thermodynamics is one of the most exciting branches of physical chemistry which has greatly contributed to the modern science. Being concentrated on a wide range of applications of thermodynamics, this book gathers a series of contributions by the finest scientists in the world, gathered in an orderly manner. It can be used in post-graduate courses for students and as a reference book, as it is written in a language pleasing to the reader. It can also serve as a reference material for researchers to whom the thermodynamics is one of the area of interest.

How to reference
In order to correctly reference this scholarly work, feel free to copy and paste the following:

Colm T. O'Mahony, Richard A. Farrell, Tandra Goshal, Justin D. Holmes and Michael A. Morris (2011). The Thermodynamics of Defect Formation in Self-Assembled Systems, Thermodynamics - Systems in Equilibrium and Non-Equilibrium, Dr. Juan Carlos Moreno PirajÃ¡n (Ed.), ISBN: 978-953-307-283-8, InTech, Available from: http://www.intechopen.com/books/thermodynamics-systems-in-equilibrium-and-non-equilibrium/the-thermodynamics-of-defect-formation-in-self-assembled-systems

INTECH
open science | open minds

InTech Europe
University Campus STeP Ri
Slavka Krautzeka 83/A
51000 Rijeka, Croatia
Phone: +385 (51) 770 447
Fax: +385 (51) 686 166
www.intechopen.com

InTech China
Unit 405, Office Block, Hotel Equatorial Shanghai
No.65, Yan An Road (West), Shanghai, 200040, China
中国上海市延安西路65号上海国际贵都大饭店办公楼405单元
Phone: +86-21-62489820
Fax: +86-21-62489821

IntechOpen